Neural Substrates of Dynamic Object Occlusion

Sarah M. Shuwairi[1], Clayton E. Curtis[1], and Scott P. Johnson[2]

Abstract

■ In everyday environments, objects frequently go out of sight as they move and our view of them becomes obstructed by nearer objects, yet we perceive these objects as continuous and enduring entities. Here, we used functional magnetic resonance imaging with an attentive tracking paradigm to clarify the nature of perceptual and cognitive mechanisms subserving this ability to fill in the gaps in perception of dynamic object occlusion. Imaging data revealed distinct regions of cortex showing increased activity during periods of occlusion relative to full visibility. These regions may support active maintenance of a representation of the target's spatiotemporal properties ensuring that the object is perceived as a persisting entity when occluded. Our findings may shed light on the neural substrates involved in object tracking that give rise to the phenomenon of object permanence. ■

INTRODUCTION

When viewing a moving object, information for the object's existence and speed are available directly, and the time the object will arrive at a particular location can be estimated by extrapolating its trajectory (McBeath, Shaffer, & Kaiser, 1995). These estimates can be updated continually based on visible information. When tracking a moving object that becomes temporarily hidden, however, its persistence, speed, and arrival time must be inferred based on information that is necessarily based on a mental representation of the object's continued existence and its trajectory. In the real world, objects move in and out of our view, and parts of objects are often hidden by surfaces of the same object or by other nearby objects. Yet, seemingly without any effort, the visual system fills in the gaps, and our perception of static and moving objects remains uninterrupted despite occlusion (Nakayama, He, & Shimojo, 1995; Michotte, Thinès, & Crabbé, 1991), even when up to four targets are tracked simultaneously (Scholl & Pylyshyn, 1999; Pylyshyn & Storm, 1988).

We reasoned that we would be able to isolate the neural correlates of dynamic object occlusion by comparing cortical activity as observers viewed a dynamic occlusion stimulus (i.e., a moving object that becomes temporarily hidden) to activity when viewing a moving, fully visible object. Participants in our task were asked to estimate the arrival time of a moving object at a prespecified location in the display as cortical activity was recorded using functional magnetic resonance imaging (fMRI). We considered the possibility, in addition, that estimates of arrival time of a concealed object might rely on a ''time-keeping'' strategy, rather than a mental representation of object persistence and speed. To distinguish a time-keeping strategy from true object tracking, we compared activation patterns as observers viewed a dynamic occlusion display to activity when viewing a stimulus in which a moving object went out of sight and back into view via shrinking and expansion. This means of disappearance/reappearance has been shown to disrupt perception of object persistence when observers track multiple targets in occlusion displays (Scholl & Pylyshyn, 1999). Perception of persistence is maintained by accretion and deletion of objects by an occluding or virtual surface, a means of disappearance/reappearance that is thought to have greater ''ecological validity'' (Gibson, 1979).

We used fMRI to measure brain activity as observers maintained central fixation and covertly tracked a visual target translating continuously and repetitively on a constant linear trajectory in three types of trial (unoccluded, occluded, and shrinking; see Figure 1). Observers' estimates of target arrival time at a specified location in the stimulus, indicated by a vertical dotted line, were recorded with a button-press task. In the unoccluded condition, we hypothesized that performance would be based on information available directly in the stimulus. In the occluded condition, we hypothesized that observers would rely on an internal representation of target persistence and trajectory when estimating arrival time. The shrinking condition, in contrast, was not expected to involve a stable representation of a persisting object, and we hypothesized that observers would employ a non-object-based strategy, such as time-keeping, to perform accurately on the task. We predicted that

[1]New York University, [2]University of California, Los Angeles

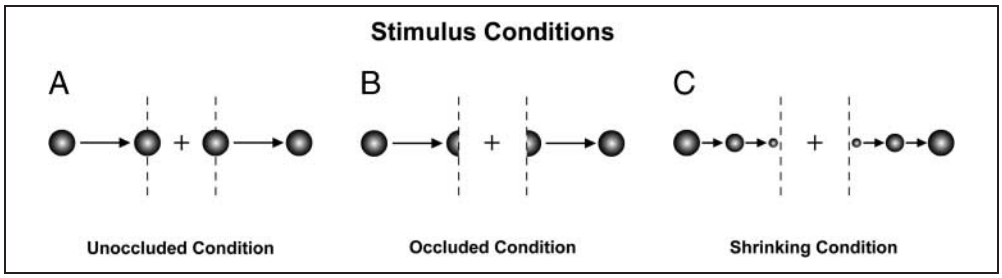

Figure 1. Schematic depictions of stimulus displays. In unoccluded trials (left), a visual target translated repetitively from left to right on a constant linear trajectory. In occluded trials (center), a portion of the target's trajectory was hidden via gradual deletion of the target by a virtual occluding surface, and revealed via gradual accretion. In shrinking trials (right), the target disappeared by imploding and reappeared by expanding on the other side. In all three types of display, a set of gray, vertical dotted lines defined a central rectangle; the rectangle defined the space in the occluded and shrinking conditions where the target was concealed and revealed.

observers would employ different cognitive strategies in each of the conditions, which, in turn, would yield differences in networks of cortical activation across the three conditions and provide evidence for the computations that subserve perception of dynamic object occlusion.

METHODS

Participants

Data from 10 participants were included in the final analysis of behavioral and brain imaging data (5 women and 5 men). Four participants were observed but excluded from the analyses because of excessive motion artifact (1 woman and 1 man), failure to understand and correctly perform the task (1 woman), or failure to complete the scanning session because of fatigue (1 man). Before scanning, all participants performed at least two practice sessions on the behavioral task. The first training session occurred several days before scanning, and the second training session occurred on the day of the scan session. During training, the experimenter instructed participants to maintain central fixation while covertly tracking the moving target and pressing a button to estimate its arrival time. Participants were instructed not to make eye movements during the task. The experimenter verified compliance by observing them during all practice trials. Voluntary written consent was obtained before testing. All aspects of the research were in compliance with safety guidelines for magnetic resonance research conducted at the Center for Brain Imaging as well as the human subjects committee (Institutional Review Board) at New York University.

Stimuli

Stimuli consisted of three types of visual display depicting a green spherical target (1° visual angle) moving horizontally across a gap (2.5° visual angle) defined by vertical gray dotted lines (Figure 1). In unoccluded trials, the target remained visible throughout the trial (Figure 1, left). In occluded trials, an invisible occluder between the dotted lines temporarily concealed the target in the center of its trajectory in an ecologically valid manner, via accretion and deletion of its visible surface (Figure 1, center). In shrinking trials, the target imploded at the first set of dotted lines and expanded on the second, an ecologically invalid means of going out of and back into view (Figure 1, right). The target moved at 2°/sec, taking 6 sec to move from left to right and 6 sec to move back. All stimuli were created using Flash (Macromedia Studio MX 2004) and exported as QuickTime movies.

A run consisted of eight repetitions of each of the three trial types. Each run began with a 4-sec central fixation and lasted 5 min 40 sec. Within each run, stimuli were presented in a predetermined pseudorandom sequence and were counterbalanced for left-right direction of movement. Each stimulus was preceded by a 2-sec interstimulus interval consisting of a centrally located fixation cross (0.25° visual angle) against a black background.

Behavioral Task

Reaction times were recorded with a magnetic resonance-compatible fiber-optic button-press instrument inside the scanning module. Individuals were instructed to press down when the target's leading edge reached the first dotted line and to release when the target's leading edge reached the second dotted line. In occluded trials, therefore, observers judged the target's impending reemergence from behind the occluding surface, and in shrinking trials, observers judged when the target would begin to expand. All participants completed one practice run immediately before scanning and three experimental runs during the scan session, which were included in the final analysis of behavioral data. Each participant contributed at least 65 data points (a minimum of 45% of all possible observations).

Functional Magnetic Resonance Imaging Data Acquisition and Analyses

Brain activity was measured with fMRI as observers participated in the behavioral task. Magnetic resonance

scanning was performed in a 3-T Siemens head-only research scanner equipped with a Siemens 3T Allegra whole-brain surface head coil. All testing was conducted in one session that consisted of structural anatomical scans and blood oxygenation level-dependent functional scans for each subject. Each scanning session began by acquiring a set of low-resolution images in the sagittal, axial, and coronal planes that were used for slice selection. A set of structural images was acquired using a T1-weighted spin echo pulse sequence (32 slices, 3 mm, TR = 600 msec, TE = 9.1 msec, total duration = 3 min 18 sec). Then a set of 3-D high-resolution magnetization prepared rapid acquisition gradient-echo images was acquired (176 slices, 1 mm, TR = 2500 msec, TE = 4.38 msec, total duration = 10 min 42 sec). A series of functional scans were performed using a standard gradient-recalled echo-planar imaging blood oxygenation level-dependent pulse sequence using the same slice orientation prescription as the T1-weighted structural scan (32 slices, 3 mm, TR = 2000 msec, TE = 30 msec, flip angle = 80°, total duration = 5 min 40 sec). The functional data were coregistered to the T1-weighted in-plane anatomical images, which were then coregistered to the high-resolution images for ensuing data analysis.

Analysis of imaging data was carried out using FEAT (fMRI Expert Analysis Tool) Version 5.1, part of FSL (Smith et al., 2004; www.fmrib.ox.ac.uk/fsl) and MRIcro (Rorden & Brett, 2000). Caret was used for 3-D rendering and optimal visualization of statistical parametric maps of activation (Van Essen, 2002; Van Essen et al., 2001; http://brainmap.wustl.edu/caret). The model used a gamma function for convolving the hemodynamic response (phase = 0, *SD* = 3 sec, lag = 6 sec). Preprocessing procedures include stripping the anatomical images of the nonbrain structures (BET), motion correction (MCFLIRT), and temporal high-pass filtering (42 sec cutoff). Statistical images were thresholded using clusters determined by a gaussian $Z > 3.0$ and a corrected cluster significance threshold of $p > .001$. Statistical maps of activation differences were plotted in contrast comparisons between each of the three conditions (unoccluded, occluded, and shrinking). Functional imaging data from each individual were coregistered to his/her own anatomical images (initial T1-weighted and 3-D high-resolution structural images), which then were coregistered to the MNI standard brain template for a group analysis.

RESULTS

Behavioral Data

Data consisted of latency differences between the observers' judgments of target arrival versus the actual time of target arrival. Results of a one-way analysis of variance yielded a reliable effect of trial type on differences in accuracy judgments of the target's arrival in each of the three conditions [mean (*SD*): unoccluded = 75.5 (111.5) msec, occluded = −53.6 (81.2) msec, shrinking = −3.2 (88.8) msec], $F(2,18) = 12.89, p < .001$]. Simple effects tests comparing pairs of trial types revealed reliable differences in all three contrasts (unoccluded vs. occluded, $p < .01$; unoccluded vs. shrinking, $p < .01$; unoccluded vs. shrinking, $p < .05$). Participants were highly engaged in tracking the stimulus in all three conditions, and accuracy was high (i.e., within 80 msec on average of the correct response). Nevertheless, there were reliable differences in mean latency of response between conditions, which supports our prediction that the three conditions evoked different cognitive operations or strategies for object tracking.

Neuroimaging Data

Group analysis of imaging data revealed a network of regions differentially involved in the three types of object tracking conditions. Unless noted otherwise, all cortical activations reported were bilateral, although there were generally more clusters of activation in the right hemisphere. Minimum cluster size is 5 voxels for reported regions of interest. Contrast comparisons between unoccluded, occluded, and shrinking conditions yielded increased neural responses in all 10 participants in a network of cortical regions ($Z > 3, p < .001$). Cortical activation differences resulting from these contrast comparisons are depicted in Figures 2–4 and are listed in detail with *xyz* coordinates in MNI space in Appendix 1.

The contrast of occluded > unoccluded (Figure 2, blue tones) was designed to isolate cognitive processes involved in tracking a target through space and time during periods of invisibility relative to full visibility. This contrast yielded activation differences in the inferior temporal cortex (lateral/superior region of fusiform and lingual gyri, Brodmann's area [BA] 27/37), posterior and anterior regions of middle and superior temporal cortex (BA 21/22/38/48), insula (BA 48), cuneus (BA 18), inferior parietal lobule (BA 39/40), midbrain regions (hippocampus, thalamus, caudate, and putamen), the cerebellum, the precentral sulcus (BA 6), and several regions of prefrontal cortex (anterior dorsolateral prefrontal regions, BA 10/46, ventrolateral prefrontal regions, BA 11/44/45/47, and along the medial wall in the superior frontal cortex in pre-supplementary motor area [SMA] and anterior cingulate, BA 6/8/32). The most robust activation differences were found in four areas: (1) inferior parietal lobule, (2) superior temporal sulcus, (3) pre-SMA, and (4) precentral sulcus. Conversely, a contrast of unoccluded > occluded (Figure 2, orange-yellow tones) was designed to isolate processes involved in tracking a target through space and time during periods of full visibility relative to invisibility. This contrast yielded activation differences in inferior

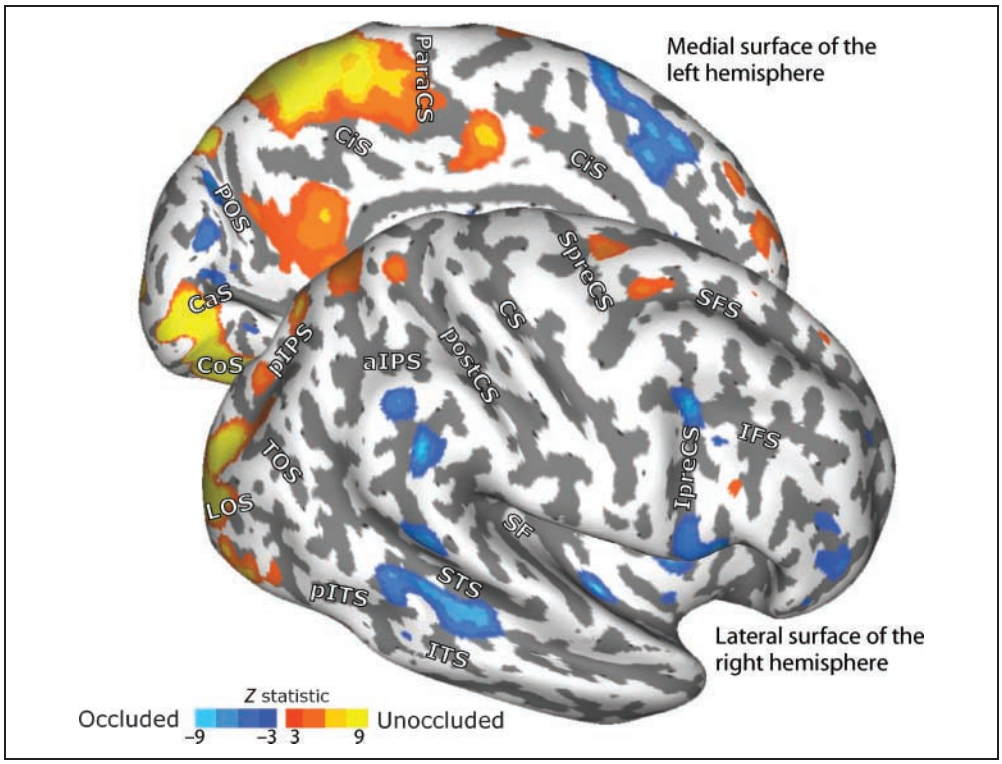

Figure 2. Contrast comparisons between unoccluded and occluded conditions projected on a slightly inflated rendering of the gray-white matter boundary of a brain in MNI stereotactic space ($n = 10$, $Z > 3, p < .001$). The dark gray color on the surface demarks sulci, and the light gray color represents gyri. Abbreviations: LOS = lateral occipital sulcus; CoS = collateral sulcus; CaS = calcarine sulcus; TOS = transverse occipital sulcus; ITS = inferior temporal sulcus; STS = superior temporal sulcus; SF = sylvian fissure; pIPS = posterior intraparietal sulcus; aIPS = anterior intraparietal sulcus; postCS = postcentral sulcus; SpreCS = superior precentral sulcus; IpreCS = inferior precentral sulcus; SFS = superior frontal sulcus; IFS = inferior frontal sulcus; CiS = cingulate sulcus; ParaCS = paracentral sulcus.

and midoccipital regions of extrastriate cortex (BA 18/19), inferior temporal cortex (medial/ventral region of fusiform gyrus, BA 37), superior parietal lobe near the posterior IPS (BA 5/7), and superior frontal sulcus (BA 6).

A contrast comparison of unoccluded > shrinking (Figure 3, orange-yellow tones) was designed to isolate processes involved in tracking a fully visible target over a period relative to tracking a target undergoing an ecologically invalid means of disappearing and reappearing. Results of this contrast yielded activation differences in the inferior and midoccipital regions of extrastriate cortex (BA 18/19), inferior temporal cortex (fusiform

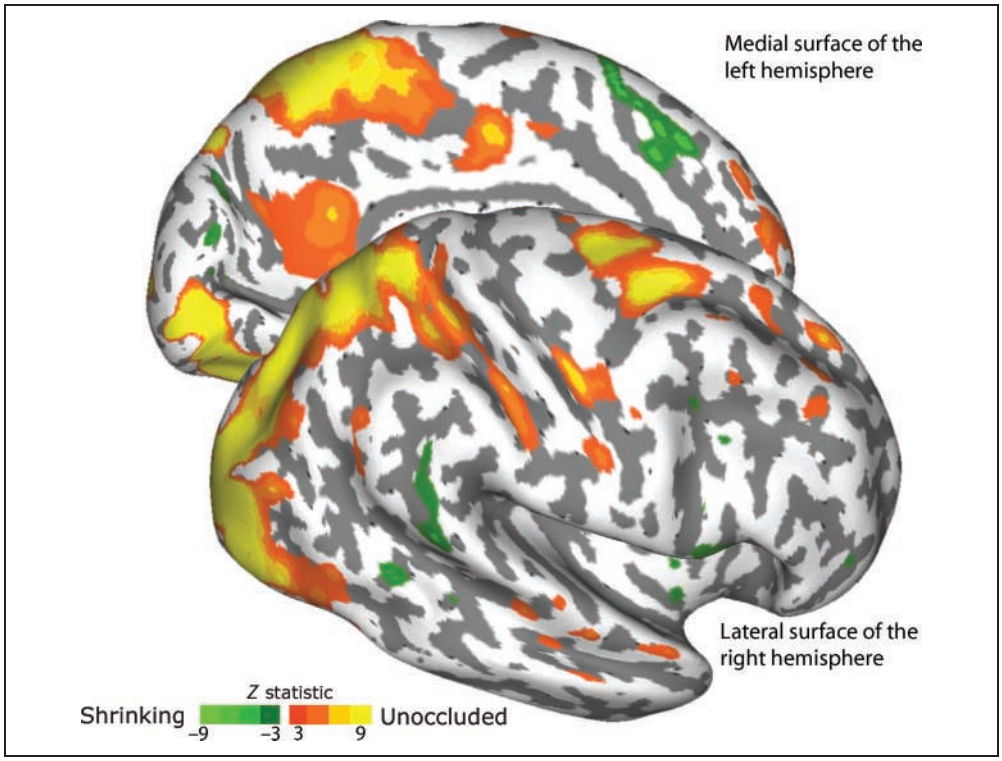

Figure 3. Contrast comparisons between unoccluded and shrinking conditions projected on a slightly inflated rendering of the gray-white matter boundary of a brain in MNI stereotactic space ($n = 10$, $Z > 3, p < .001$).

gyrus, BA 37), hippocampus and parahippocampal cortex, middle and superior temporal cortex (BA 21/22/48 and left BA 38), superior parietal lobe (BA 5/7) as well as in the superior and midorbital prefrontal regions (BA 6, BA 9, BA 9/46/45, BA 10, and left BA 9/32). A contrast of shrinking > unoccluded (Figure 3, green tones) was designed to isolate processes involved in tracking a moving target undergoing an ecologically invalid means of disappearing and reappearing relative to tracking a fully visible target over a period. Results of this contrast yielded activation differences in the cuneus (BA 18), lingual gyrus (BA 37), medial frontal cortex in pre-SMA and anterior cingulate (BA 6/8/32), inferior frontal gyrus (BA 45/47), and right temporal cortex (BA 21/22).

The contrast comparison of occluded > shrinking (Figure 4, blue tones) was designed to isolate cognitive processes involved in tracking a moving object through space and time during periods of invisibility relative to tracking a moving target undergoing an ecologically invalid means of disappearance/reappearance. Results of this comparison yielded activation differences in the superior and midoccipital cortex (BA 18/19) including the cuneus (medial BA 18), superior parietal lobule (BA 5/7) including the precuneus (BA 5), inferior temporal cortex (BA 37), middle and superior temporal cortex (BA 21/22/48), insula (BA 48), midbrain regions including the hippocampus and parahippocampus (BA 27/30/37), thalamus, caudate, and putamen, as well as in frontal regions of cortex in the precentral and postcentral sulcus (BA 4/6), superior frontal cortex (BA 9), dorsolateral prefrontal cortex (BA 45/46), and right mid-orbito-frontal cortex (BA 10/11/47). Interestingly, the contrast of shrinking > occluded (Figure 4, green tones) yielded no voxels showing greater activation in shrinking relative to occluded trials.

DISCUSSION

Maintenance of object representations across temporary gaps in space and time might comprise a combination of lower and higher perceptual and cognitive mechanisms. We used an object tracking task and functional neuroimaging to begin to clarify these mechanisms, in part by distinguishing them from mechanisms involved in tracking fully visible objects and from mechanisms involved in estimating a simple temporal gap. Results from our behavioral task demonstrated that observers were engaged in the tracking task. Judgments of target arrival time were reliably different across conditions, suggesting that the three tasks evoked a different cognitive state, mental operation, or strategy to perform as accurately as possible in each separate condition. When the target was fully visible, judgments of target arrival time tended to be late, implying a strategy in which observers tracked the visible motion and initiated a button press as the target reached the appropriate location. When the target was occluded, judgments of target arrival time tended to be early, suggesting that observers anticipated its arrival and did not wait to press when it reappeared, which would have led to a longer latency. This suggests

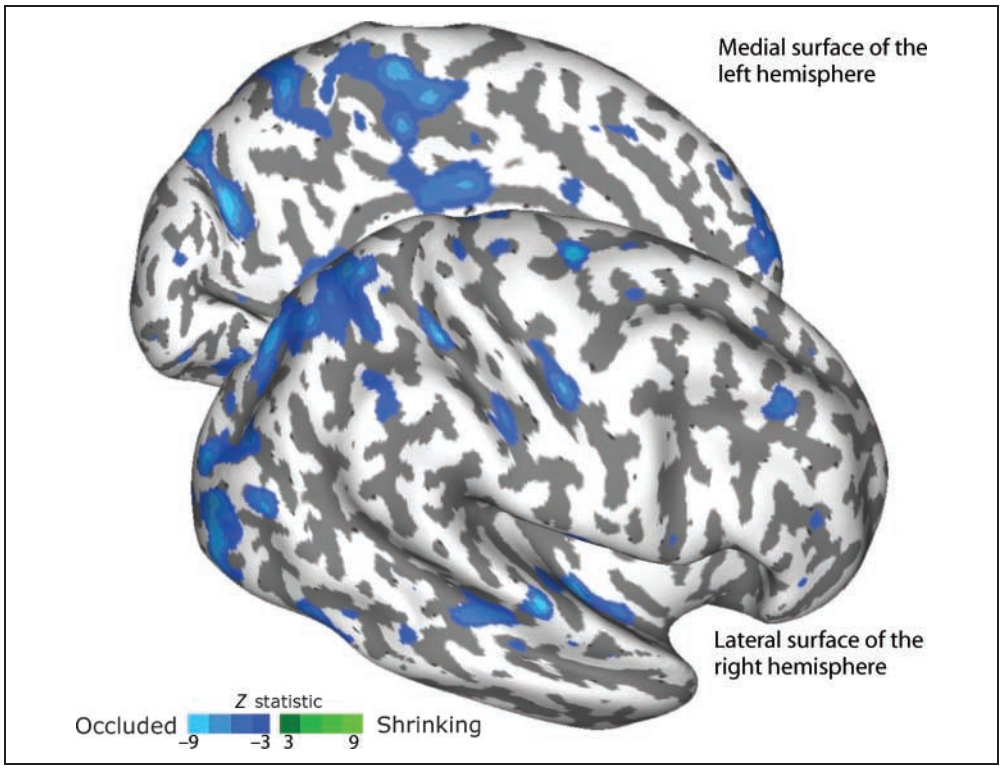

Figure 4. Contrast comparisons between occluded and shrinking conditions projected on a slightly inflated rendering of the gray-white matter boundary of a brain in MNI stereotactic space ($n = 10$, $Z > 3$, $p < .001$).

that observers maintained a representation of the spatiotemporal information during occlusion and interpolated the invisible motion of the target. Our intuitions of a time-keeping strategy in the shrinking condition were supported anecdotally: Several observers reported that they employed a ''counting'' strategy in which they simply tried to time the reemergence from learning the timing and counting to themselves after the target imploded.

The unoccluded > occluded and unoccluded > shrinking contrasts yielded increased activation in extrastriate (occipital, inferior temporal, and posterior parietal) visual cortical areas. This is not surprising given that in unoccluded trials observers tracked a continuously visible target object moving in a constant trajectory. Increased activation in these regions of extrastriate cortex has been previously reported during conditions of attentive tracking relative to passive viewing of multiple moving objects (Culham, Cavanagh, & Kanwisher, 2001; Culham et al., 1998). The occluded > unoccluded contrast yielded increased activation in the precentral sulcus, inferior parietal lobule, temporal cortex, and prefrontal cortical regions along the dorsal medial wall. Notably, almost identical foci in the precentral sulcus and inferior parietal lobule show an attentive tracking load effect (i.e., activation increases with the number of moving items that are simultaneously tracked) (Culham et al., 2001). Moreover, these same areas also activate during tasks of visual working memory (Courtney, Ungerleider, Keil, & Haxby, 1997) and sustained visual attention (Serences & Yantis, 2007). The occluded > shrinking contrast yielded increased bilateral activation in lateral occipital cortex (LOC) that may have been evoked by the continued representation of the object. Consistent with this interpretation, several other neuroimaging studies also report increased neural activity in LOC during tasks of form perception and object recognition (Lerner, Hendler, & Malach, 2002; Malach et al., 1995), illusory contours (Ffytche & Zeki, 1996; Hirsch et al., 1995), and perceptual completion of static surfaces (Stanley & Rubin, 2003; Mendola, Dale, Fischl, Liu, & Tootell, 1999). In all comparisons against unoccluded, we found increased activation in the pre-SMA. Past studies have found increased activation in this area when an internal representation of time must be maintained (e.g., estimating a length of time or the timing of a motor response).

Maintaining active representations of objects through occlusion is likely accomplished by a combination of mechanisms such as perceptual completion (Nakayama et al., 1995), selective attention (Scholl, 2001; Awh, Jonides, & Reuter-Lorenz, 1998), and visual working memory (Pasternak & Greenlee, 2005). Moreover, mechanisms supporting inferred motion and trajectory extrapolation (Barborica & Ferrera, 2003; Assad & Maunsell, 1995) and preparatory oculomotor behaviors (Curtis, 2006; Curtis & D'Esposito, 2006a; Curtis, Rao, & D'Esposito, 2004) constantly update the visual system with the moving target's changing location in space. These mechanisms may work in unison to maintain a representation of the moving object in space and time despite perceptual interference such as occlusion.

Selective attention may serve as a crucial higher order mechanism that facilitates representations of dynamic object occlusion in visual working memory. Increased responses in posterior parietal cortex have been associated with maintaining the locus of visuospatial attention in working memory (Serences & Yantis, 2007; Todd & Marois, 2004), and the overall magnitude of posterior parietal activation may be an indicator of observers' visual working memory capacity (Xu & Chun, 2006; Todd & Marois, 2005). In addition, several frontal, posterior parietal, and temporal cortical areas show evidence of persistent activity during delay periods when observers maintain a representation of an object or its position in working memory (Curtis & D'Esposito, 2006b). Therefore, the activations associated with attentive tracking through occlusion that we report here may reflect some of the same mechanisms that support maintenance of an object's spatiotemporal information in visual working memory.

A recent study compared human parietal cortex activation during an occlusion task relative with a condition in which the object simply blinked out of existence (Olson, Gatenby, Leung, Skudlarski, & Gore, 2003). The authors found that a portion of the posterior parietal cortex, bilaterally, showed a greater response during occlusion. We report here that what appears to be the same portion of the parietal cortex showed greater activation during occlusion than shrinking. This activation may reflect the activity of neurons in posterior parietal cortex that are motion sensitive and increase their rates of firing during a period when a moving object is briefly occluded (Assad & Maunsell, 1995). Therefore, the posterior parietal cortex may be involved in processing spatiotemporal properties, including the inferred motion, of objects. Moreover, we extend the results of Olson et al. (2003) by demonstrating that the posterior parietal cortex is only one part of a larger neural network that also includes LOC, superior temporal, superior frontal, and premotor cortices, which, together, are involved in tracking objects through occlusion.

Together with findings from past research, our results shed light on the precise nature of dynamic object occlusion. Cortical networks involved in perceptual completion, visual working memory, motion perception, and timing estimation work in concert to yield representations of moving objects under conditions of concealment. These networks appear to be invoked uniquely during invisible object tracking, as opposed to similar tasks, one involving full visibility and the other an ecologically invalid means of invisibility. Perception of dynamic object occlusion, therefore, would appear to comprise a distinct cognitive operation that is observable with functional neuroimaging techniques.

APPENDIX 1. REGIONS YIELDING SIGNIFICANT ACTIVATION DIFFERENCES IN CONTRAST COMPARISONS

	Left Hemisphere				*Right Hemisphere*			
	Maximum Z Score	*x*	*y*	*z*	*Maximum Z Score*	*x*	*y*	*z*
Unoccluded > occluded								
Extrastriate regions								
Inferior occipital (BA 18/19)	10.19	−12	−96	−6	12.69	18	−94	2
Superior parietal (BA 7)	5.67	−28	−52	60	5.94	26	−58	64
Precuneus (BA 5)	5.16	0	−61	58	4.68	10	−53	59
Temporal regions								
Fusiform gyrus (BA 37)	7.78	−31	−59	−16	5.25	26	−56	−16
Frontal regions								
Superior frontal sulcus (BA 6)	6.68	−22	−12	58	5.26	22	−8	52
Occluded > unoccluded								
Extrastriate regions								
Inferior parietal, supramarginal gyrus (BA 40)	6.75	−52	−46	34	6.89	64	−46	39
Inferior parietal, angular gyrus (BA 39)	3.92	−38	−52	32	6.80	52	−60	48
Cuneus (BA 18)	6.80	−9	−83	15	4.50	9	−84	15
Superior cerebellar vermis	5.60	−8	−48	−20	5.62	10	−58	−8
Temporal regions								
Inferior temporal (BA 37)	3.87	−42	−34	−14	4.44	50	−45	−15
Fusiform gyrus (BA 37)	4.25	−16	−38	−14	5.20	40	−29	−14
Lingual gyrus (BA 27/37)	4.44	−26	−52	−1	4.44	24	−45	−4
Midtemporal gyrus (BA 21/22)	7.74	−48	−34	0	7.71	66	−38	6
Posterior superior temporal (BA 22)	4.91	−60	−47	14	7.18	54	−16	4
Anterior superior temporal (BA 22/48)	5.63	−44	4	−12				
Rolandic operculum (BA 48)	5.59	−54	9	6				
Temporal pole (BA 38)	5.35	−44	8	−18	6.00	36	16	−20
Anterior insula (BA 48)	6.90	−40	2	2	6.76	32	−21	20
Midbrain regions								
Thalamus	8.84	−16	−22	20	8.97	11	−19	18
Caudate	6.52	−8	16	5	6.28	6	16	4
Putamen	6.77	−30	−11	−4	4.72	34	−3	0
Hippocampus	5.00	−12	−34	5	6.61	20	−4	−12
Amygdala	4.96	−31	−6	−14	6.22	30	−6	−12

APPENDIX 1 (*continued*)

	Left Hemisphere				*Right Hemisphere*			
	Maximum Z Score	*x*	*y*	*z*	*Maximum Z Score*	*x*	*y*	*z*
Frontal regions								
Precentral sulcus (BA 6)	6.73	−34	−1	38				
Superior medial frontal (pre-SMA, BA 6/8)	4.58	−1	20	60	8.17	8	16	62
Dorsal anterior cingulate (BA 32)	6.57	−12	−14	48	6.54	7	36	42
Anterior cingulate (BA 32/24)	4.87	−1	20	40	6.05	10	24	40
Superior medial frontal (BA 10)	4.44	−18	50	14	6.33	20	44	8
Dorsal lateral frontal (BA 10/46)	3.66	−20	45	16	6.33	40	50	−2
Inferior prefrontal (BA 45)	4.72	−50	40	−2	8.55	50	38	2
Lateral orbito-frontal (BA 47)	8.27	−34	40	−12	8.31	48	38	−8
Medial orbito-frontal (BA 11)	6.14	−17	38	−10	7.70	22	36	−9
Inferior frontal (BA 44)	5.16	−50	10	14	3.90	53	11	14
Unoccluded > shrinking								
Extrastriate regions								
Occipital (BA 18/19)	11.36	−12	−96	−8	13.00	14	−88	−10
Superior parietal (BA 7)	9.26	−20	−66	66	8.85	26	−60	66
Precuneus (BA 5/7)	8.04	−1	−66	54	9.06	2	−66	54
Temporal regions								
Fusiform gyrus (BA 37)	11.41	−28	−50	−18	8.65	30	−50	20
Middle temporal gyrus (BA 21)	5.58	−50	−2	−14	7.68	64	−4	−20
Superior temporal sulcus (BA 22/48)	4.91	−48	−18	−6	6.71	56	−4	−12
Posterior superior temporal gyrus (BA 22/48)	5.99	−48	−15	0	6.81	64	0	−4
Superior temporal pole (BA 38)	4.81	−50	14	−22				
Midbrain regions								
Hippocampus/parahippocampus	9.88	−22	−32	−6	9.01	22	−32	−6
Frontal regions								
Superior precentral sulcus (BA 6)	8.16	−20	−2	60	8.25	26	−12	55
Dorsal lateral prefrontal (BA 9/46/45)	4.13	−31	30	36	6.38	28	36	28
Dorsal medial frontal (BA 9/32)	8.63	−12	41	38				
Frontal pole (BA 9/10)	6.00	−1	52	30	6.24	4	52	44
Shrinking > unoccluded								
Extrastriate regions								
Cuneus (BA 18)	5.74	−4	−89	20	4.07	9	−80	28
Lingual gyrus (BA 27/37)	5.39	−26	−50	0	6.21	36	−51	4

APPENDIX 1 (*continued*)

	Left Hemisphere				*Right Hemisphere*			
	Maximum Z Score	*x*	*y*	*z*	*Maximum Z Score*	*x*	*y*	*z*
Temporal regions								
Superior temporal gyrus (BA 22)					3.40	59	−50	22
Middle temporal gyrus (BA 21)					6.01	60	−44	12
Frontal regions								
Dorsal medial frontal (pre-SMA, BA 6/8)	4.67	−1	19	58	8.34	9	16	62
Dorsal anterior cingulate (BA 32)	6.34	−14	26	40	6.14	8	34	42
Inferior frontal (BA 45/47)	4.2	−42	50	2	8.41	50	38	2
Occluded > shrinking								
Extrastriate regions								
Occipital (BA 18/19)	5.78	−38	−89	7	7.41	46	−83	14
Cuneus (medial BA 18)	4.54	−10	−72	32	5.60	17	−70	25
Precuneus (BA 5)	6.02	−1	−38	61	6.70	2	−38	60
Lateral superior parietal (BA 7)	6.17	−20	−66	66	5.87	36	−58	62
Temporal regions								
Fusiform gyrus (BA 37)	5.74	−26	−48	−18	5.77	28	−42	−16
Medial middle temporal (BA 21)	6.04	−47	−36	0	6.80	43	−42	8
Lateral middle temporal (BA 22)					5.56	63	−37	4
Lateral superior temporal (BA 22/48)	7.12	−63	−13	4	5.49	54	−18	5
Medial superior temporal (BA 22)					5.76	46	−18	0
Superior temporal sulcus (BA 48)	5.71	−40	−8	−11	6.84	44	−16	−2
Rolandic Operculum (BA 48)	5.35	−39	−20	20	4.69	44	−21	20
Insula (BA 48)	6.63	−42	−9	10	6.52	38	6	−11
Midbrain regions								
Hippocampus/parahippocampus (BA 30/37)	6.56	−20	−38	8	7.52	26	−38	−8
Thalamus	6.55	−18	−20	16	6.80	20	−20	17
Caudate	5.46	−2	14	5	5.28	6	16	4
Putamen	8.05	−24	−2	12	6.27	28	18	0
Frontal regions								
Postcentral sulcus (BA 4)					6.95	52	−16	48
Superior frontal gyrus and precentral sulcus (BA 6)					5.17	44	0	40
Precentral sulcus (BA 6/4)	6.87	−22	−16	52	5.03	35	−19	50
Supplementary motor area (BA 4/6)	5.99	−12	−2	50	3.79	6	−21	52

APPENDIX 1 (*continued*)

	Left Hemisphere				*Right Hemisphere*			
	Maximum Z Score	*x*	*y*	*z*	*Maximum Z Score*	*x*	*y*	*z*
Dorsal medial superior frontal (BA 9)	4.11	−21	37	36	5.88	5	54	42
Dorsal anterior cingulate (BA 32)	8.49	−14	−26	48				
Dorsal lateral prefrontal (BA 46)	5.99	−14	36	30	5.35	28	36	26
Frontal pole (BA 10)					5.10	20	52	7
Lateral orbito-frontal (BA 11/47)					5.60	26	45	−8
Midlateral prefrontal (BA 45)	5.49	−42	33	36	4.78	46	44	23

Acknowledgments

We thank the MRI Users Group at New York University for helpful suggestions during earlier stages of this research and Dorothy Schirkofsky for programming the original experiment. S. M. S. thanks David Heeger and Souheil Inati for discussions of experimental design and data analysis. This research was supported in part by federal funds from national Institutes of Health (R01-HD40432 and R01-HD048733) and National Science Foundation (BCS-0418103) to S. P. J. and from The Beatrice and Samuel A. Seaver Foundation administered by the Center for Brain Imaging at New York University to S. M. S.

Reprint requests should be sent to Sarah M. Shuwairi, Department of Psychology, New York University, 6 Washington Place, New York, NY 10003, or via e-mail: sms425@nyu.edu, or to Scott P. Johnson, Department of Psychology and Center for Neural Science, New York University, 6 Washington Place, New York, NY 10003, or via e-mail: scott.johnson@nyu.edu.

REFERENCES

Assad, J. A., & Maunsell, J. H. R. (1995). Neuronal correlates of inferred motion in primate posterior parietal cortex. *Nature, 373,* 518–521.

Awh, E., Jonides, J., & Reuter-Lorenz, P. A. (1998). Rehearsal in spatial working memory. *Journal of Experimental Psychology: Human Perception and Performance, 24,* 780–790.

Barborica, A., & Ferrera, V. P. (2003). Estimating invisible target speed from neuronal activity in monkey frontal eye field. *Nature Neuroscience, 6,* 1–9.

Barborica, A., & Ferrera, V. P. (2004). Modification of saccades evoked by stimulation of frontal eye field during invisible target tracking. *Journal of Neuroscience, 24,* 3260–3267.

Bruce, C. J., & Goldberg, M. E. (1985). Primate frontal eye fields: I. Single neurons discharging before saccades. *Journal of Neurophysiology, 53,* 603–635.

Courtney, S. M., Ungerleider, L. G., Keil, K., & Haxby, J. V. (1997). Transient and sustained activity in a distributed neural system for human working memory. *Nature, 386,* 608–611.

Culham, J. C., Brandt, S. A., Cavanagh, P., Kanwisher, N. G., Dale, A. M., & Tootell, R. B. H. (1998). Cortical fMRI activation produced by attentive tracking of moving targets. *Journal of Neurophysiology, 80,* 2657–2670.

Culham, J. C., Cavanagh, P., & Kanwisher, N. G. (2001). Attention response functions: Characterizing brain areas using fMRI activation during parametric variations of attentional load. *Neuron, 32,* 737–745.

Curtis, C. E. (2006). Prefrontal and parietal contributions to spatial working memory. *Neuroscience, 139,* 173–180.

Curtis, C. E., & D'Esposito, M. (2006a). Selection and maintenance of saccade goals in the human frontal eye fields. *Journal of Neurophysiology, 95,* 3923–3927.

Curtis, C. E., & D'Esposito, M. (2006b). Functional neuroimaging of working memory. In R. Cabeza & A. Kingstone (Eds.), *Handbook of functional neuroimaging of cognition* (2nd ed., pp. 269–306). Cambridge: MIT Press.

Curtis, C. E., Rao, V. Y., & D'Esposito, M. (2004). Maintenance of spatial and motor codes during oculomotor delayed response tasks. *Journal of Neuroscience, 241,* 3944–3952.

Ffytche, D. H., & Zeki, S. (1996). Brain activity related to the perception of illusory contours. *Neuroimage, 3,* 104–108.

Gibson, J. J. (1979). *The ecological approach to visual perception.* Boston: Houghton Mifflin.

Hirsch, J., DeLaPaz, R. L., Relkin, N. R., Victor, J., Kim, K., Li, T., et al. (1995). Illusory contours activate specific regions in human visual cortex: Evidence from functional magnetic resonance imaging. *Proceedings of the National Academy of Sciences, U.S.A., 92,* 6469–6473.

Lerner, Y., Hendler, T., & Malach, R. (2002). Object completion effects in the human lateral occipital complex. *Cerebral Cortex, 12,* 163–177.

Livesey, A. C., Wall, M. B., & Smith, A. T. (2007). Time perception: Manipulation of task difficulty dissociates clock functions from other cognitive demands. *Neuropsychologia, 45,* 321–331.

Malach, R., Reppas, J. B., Benson, R. R., Kwong, K. K., Jiang, H., Kennedy, W. A., et al. (1995). Object-related activity revealed by functional magnetic resonance imaging in human occipital cortex. *Proceedings of the National Academy of Sciences, U.S.A., 92,* 8135–8139.

McBeath, M. K., Shaffer, D. M., & Kaiser, M. K. (1995). How baseball outfielders determine where to run to catch fly balls. *Science, 268,* 569–573.

Mendola, J. D., Dale, A. M., Fischl, B., Liu, A. K., & Tootell, R. B. (1999). The representation of illusory and real contours in human cortical visual areas revealed by functional magnetic resonance imaging. *Journal of Neuroscience, 19,* 8560–8572.

Michotte, A., Thinès, G., & Crabbé, G. (1991). Amodal completion of perceptual structures. In G. Thinès, A. Costall, & G. Butterworth (Eds.), *Michotte's experimental phenomenology of perception* (pp. 140–167). Hillsdale, NJ: Erlbaum.

Nakayama, K., He, Z. J., & Shimojo, S. (1995). Visual surface representation: A critical link between lower-level and higher-level vision. In S. M. Kosslyn & D. N. Osherson (Eds.), *Visual cognition: An invitation to cognitive science* (2nd ed., vol. 2, pp. 1–70). Cambridge: MIT Press.

Olson, I. R., Gatenby, J. C., Leung, H. C., Skudlarski, P., & Gore, J. C. (2003). Neuronal representation of occluded objects in the human brain. *Neuropsychologia, 42,* 95–104.
Pasternak, T., & Greenlee, M. W. (2005). Working memory in primate sensory systems. *Nature Reviews Neuroscience, 6,* 97–107.
Pylyshyn, Z. W., & Storm, R. W. (1988). Tracking multiple independent targets: Evidence for a parallel tracking mechanism. *Spatial Vision, 3,* 179–197.
Rorden, C., & Brett, M. (2000). Stereotaxic display of brain lesions. *Behavioural Neurology, 12,* 191–200.
Scholl, B. J. (2001). Objects and attention: The state of the art. *Cognition, 80,* 1–46.
Scholl, B. J., & Pylyshyn, Z. W. (1999). Tracking multiple items through occlusion: Clues to visual objecthood. *Cognitive Psychology, 38,* 259–290.
Serences, J. T., & Yantis, S. (2007). Representation of attentional priority in human occipital, parietal, and frontal cortex. *Cerebral Cortex, 17,* 284–293.
Smith, S. M., Jenkinson, M., Woolrich, M. W., Beckmann, C. F., Behrens, T. E. J., Johansen-Berg, H., et al. (2004). Advances in functional and structural MR image analysis and implementation as FSL. *Neuroimage, 23,* 208–219.
Stanley, D. A., & Rubin, N. (2003). fMRI activation in response to illusory contours and salient regions in the human lateral occipital complex. *Neuron, 37,* 323–331.
Todd, J. J., & Marois, R. (2004). Capacity limit of visual short-term memory in human posterior parietal cortex. *Nature, 428,* 751–754.
Todd, J. J., & Marois, R. (2005). Posterior parietal cortex activity predicts individual differences in visual short-term memory capacity. *Cognitive, Affective and Behavioral Neuroscience, 5,* 144–155.
Van Essen, D. C. (2002). Windows on the brain. The emerging role of atlases and databases in neuroscience. *Current Opinion in Neurobiology, 12,* 574–579.
Van Essen, D. C., Dickson, J., Harwell, J., Hanlon, D., Anderson, C. H., & Drury, H. A. (2001). An integrated software system for surface-based analyses of cerebral cortex. *Journal of the American Medical Informatics Association, 41,* 1359–1378.
Xu, Y., & Chun, M. M. (2006). Dissociable neural mechanisms supporting visual short-term memory for objects. *Nature, 440,* 91–95.